International Journal of Medical, Medicine and Health Sciences
ISSN: 2517-9969
Vol:12, No:9, 2018

# Multiscale Syntheses of Knee Collateral Ligament Stresses: Aggregate Mechanics as a Function of Molecular Properties

Raouf Mbarki, Fadi Al Khatib, Malek Adouni

***Abstract*****—**Knee collateral ligaments play a significant role in restraining excessive frontal motion (varus/valgus rotations). In this investigation, a multiscale frame was developed based on structural hierarchies of the collateral ligaments starting from the bottom (tropocollagen molecule) to up where the fibred reinforced structure established. Experimental data of failure tensile test were considered as the principal driver of the developed model. This model was calibrated statistically using Bayesian calibration due to the high number of unknown parameters. Then the model is scaled up to fit the real structure of the collateral ligaments and simulated under realistic boundary conditions. Predications have been successful in describing the observed transient response of the collateral ligaments during tensile test under pre- and post-damage loading conditions. Collateral ligaments maximum stresses and strengths were observed near to the femoral insertions, a results that is in good agreement with experimental investigations. Also for the first time, damage initiation and propagation were documented with this model as a function of the cross-link density between tropocollagen molecules.

***Keywords*****—**Multiscale model, tropocollagen, fibrils, ligaments.

## I. Introduction

THE knee collateral ligaments are mainly dominated by parallel-fibered collagen structure (type I) and a small percentage of proteoglycan and elastin (less than 20% of the solid) [1], [2]. The medial and lateral collateral ligaments (MCL and LCL) are considered part of the most frequently injured ligamentous structures of the knee joint [3]-[5]. The training activities involving varus/valgus knee loading such as football, hockey, and skiing, have contributed to the common occurrence of collateral ligaments injuries [6]-[8]. The biomechanical properties of the collateral ligaments have been studied in both human and animal models. In vitro study using cadaveric knees, MCL provided 60% of the restraining valgus moment at 5 degrees of knee flexion and provided 80% of the moment at 25 degrees of knee flexion [9], [10]. This was explained by the retrieved energy of the posterior capsule during knee flexion. The most intense interest in collateral ligament investigation included the structural properties, mechanical behavior, effects of immobilization, and ligamentous healing. On the mechanical behavior, MCL and anterior cruciate ligaments were characterized by the highest yield strength while LCL was the lowest in the tibiofemoral joint [10].

Several theories of increasing complexity have been proposed and used to quantitatively assess the temporal response of the collateral ligaments, especially MCL. These studies were driven by the measured data reported on these tissues. Starting from the simple monophasic linear elastic model (one-dimensional representation of the ligaments) [11] to macro nonlinear porous viscoelastic/elastic fibrils reinforced finite elements models (three-dimensional representation of the ligaments) [12] were used. These models have been quite successful in delivering the measured response under low or regular loading rate, but no single model has yet been able to describe the real complexity of the connective tissue by including the full path from elasticity to plasticity (damage). This later was linked to the fibril capacity in supporting tensile loading [1], [2]. A clear connection between fibrils micro defect and aggregate mechanics of the collateral ligaments, if identified, can help to create a clear framework for a joint loading under safe physiological conditions.

In this study, we developed a multi-scale constitutive model which considers the structural hierarchies of soft tissues [13]. This model creates a relationship driven the aggregate mechanical behavior of the soft tissues as a function of the basic nanoscale properties predicted by molecular simulations. We hypothesize that (1) multiscale fibril reinforced hyper-elastoplastic model may accurately be used to estimate transient nonlinear collateral ligaments response and (2) nonlinear properties of the ligaments alter substantially with the molecular properties changes.

## II. Method

**Constitutive model:** A multiplicative decomposition of the deformation gradient (F) into elastic ($F^e$) and plastic ($F^p$) parts is considered here to create the fiber reinforced composites model of collateral ligaments. Due to the structure and the deformation mechanisms of the soft tissues, the plastic flow is associated only with the uniaxial deformation of the fibrils ($F^f = F^p$). Therefore, the tissue is considered as hierarchical hyper-elastoplastic composite material starting from the fibril level (1 μm) to continuum macro tissue level (+100 μm). Neo-Hookean generalized strain energy is used to model the fibril

Raouf Mbarki and Fadi Alkhatib are with the Australian College of Kuwait, Mechanical Engineering department, east meshrif, Kuwait, P.O. Box 1411 (e-mail: r.mbarki@ack.edu.kw, f.alkhatib@ack.edu.kw).

Malek Adouni is with the Northwestern University, Physical Medicine and Rehabilitation Department, 345 East Superior Street, Chicago, IL 60611 & Legs + Walking Lab, Shirley Ryan AbilityLab, Chicago, IL 60611 & Australian College of Kuwait, Mechanical Engineering department, east meshrif, Kuwait, P.O. Box 1411 (corresponding author, e-mail: malek.adouni@northwestern.edu).

behavior as follows:

$$\psi_{fl}(\bar{I}_{1e}, \bar{I}_{4e}) = \frac{1}{2}\mu^{fl}(\bar{I}_{4e})(\bar{I}_{1e} - 3)$$

where $\bar{I}_{1e}$ = tr ($\bar{C}^e = \bar{F}^e\ \bar{F}^{eT}$) and $\bar{I}_{4e}$= $n_0\ \bar{C}^e\ n_0^t$ with $n_0$ is the fiber direction at the initial configuration. The shear moduli $\mu^{fl}$ is considered as a function of the elastic fibrils deformations with

$$\mu^{fl}(\bar{I}_{4e}) = \mu_0\left(tanh\left(a_1(\bar{I}_{4e} - 1)\right) - a_2 ex\,p\left(a_3(\bar{I}_{4e} - I_0)\right)\right)$$

where $\mu_0$ is the shear modulus of the fibril and $a_i$ is dimensionless fibril parameters, this hyperbolic function used to fit the stiffness evolution of the fibril predicted by molecular dynamic simulations during atomistic analyses [13], [14]. Moreover, it is postulated that the yield condition (1), the plastic strain rate (2) and the flow resistance (3) of the tissue are directly related to the effective stress of the fibrils with [15].

$$\begin{cases} \sigma_{eff} = \frac{4}{3}\bar{I}_{4e}\frac{\partial \psi_{fl}}{\partial \bar{I}_{4e}} = g_i + c\beta^2 & (1) \\ \dot{\gamma} = \dot{\gamma}_0\left|\frac{\sigma_{eff}}{\alpha(t)}\right|^{1/m} sig(\sigma_{eff}) & (2) \\ \alpha(t) = \int h\dot{\gamma} f(\alpha) & (3) \end{cases}$$

Here $g_i + c\beta^2$ represent the yield strength of the fibril which is a function of the cross-link density between tropocollagen molecules (Fig. 1). This relationship serves as the basis for the multi-scale coupling between nanoscale collagen features and materials properties at large tissues scales (Fig. 1).

The fiber of collagen (10 μm) and then the collateral ligaments (+100 μm) are modeled as depth-dependent fibril reinforced composite material with an incompressible neo-Hookean total strain energy function as follow:

$$\psi_t(\bar{I}_{1f}, \bar{I}_4, \bar{I}_{4e}) = \frac{1}{2}\bar{\mu}_m(\bar{I}_{1f} - 3) + \frac{1}{2}\bar{\mu}_{fl}(\bar{I}_{1ef} - 3) + \frac{1}{2}\bar{\mu}_{eff}(\bar{I}_1 - \bar{I}_{1f})$$

where $\bar{I}_{1f} = \bar{I}_4 + 2\,\bar{I}_4^{-1/2}$, $\bar{I}_{1ef} = \bar{I}_{e4} + 2\,\bar{I}_{e4}^{-1/2}$, $\bar{\mu}_m = v_f\, v_{fm}\, \mu_m, + v_m\, \mu_m$, $\bar{\mu}_{fl} = v_f\, v_{fl}\, \mu_{fl}$, $\mu^{eff}$ is the effective shear moduli of fibril, $v_f$ and $v_{fl}$ are volume fraction of the fiber and fibril, respectively, $\mu_m$ and $\mu_{fm}$ are the shear moduli of the matrix of the fiber and the matrix of the collateral ligaments, respectively.

By satisfying both the Clausius-Duhem dissipation inequality at the macroscopic continuum level and the constraint of the incompressibility of soft tissue, the total stress $\sigma^t$ can be expressed with fibril $\sigma^f$ and no-fibril $\sigma^{nf}$ stress tensors as follows:

$$\sigma^t = \sigma^{nf} + \sigma^f$$
$$\begin{cases} \sigma^f = \frac{2}{J}\left(\bar{I}_4\frac{\partial \psi_t}{\partial \bar{I}_4} dev(n \otimes n) + \bar{I}_{4e}\frac{\partial \psi_t}{\partial \bar{I}_{4e}} dev(n_e \otimes n_e)\right) if\ \bar{I}_{4e} > 1 \\ \sigma^f = 0\ if\ \bar{I}_{4e} \le 1 \end{cases}$$

where $n = \bar{F}\, n_0 / \left\|\bar{F}\, n_0\right\|$

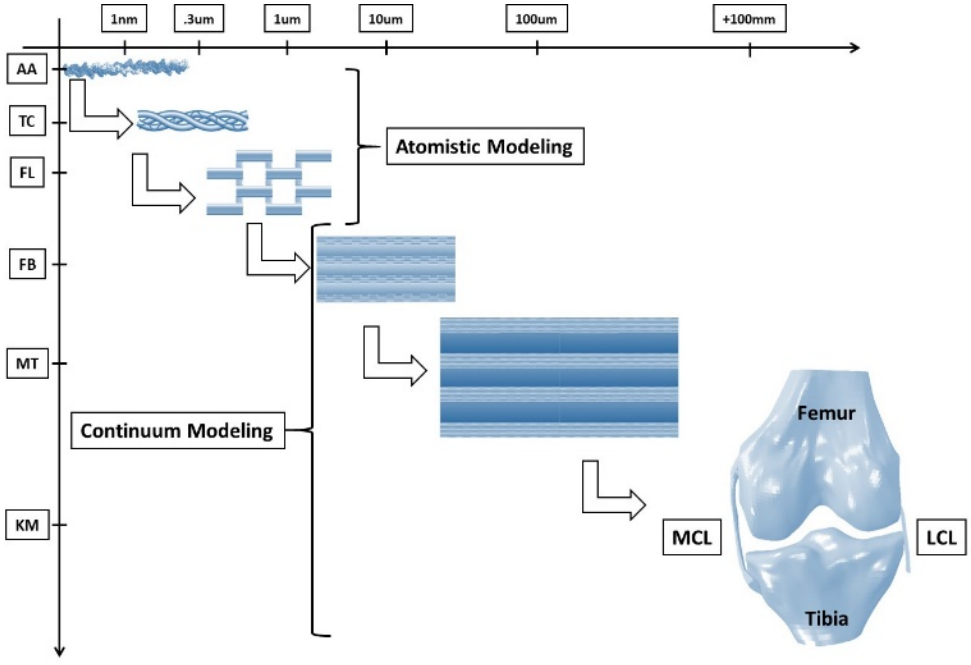


Fig. 1 Schematic view of the Hierarchical features of the multi-scale model of the articular cartilage. (AA) Amino acids, (TC) tropocollagen, (FL) Fibrils, (FB) Fibers, (MT) Macro tissue, (MCL and LCL) collateral ligaments of the knee model

MCL

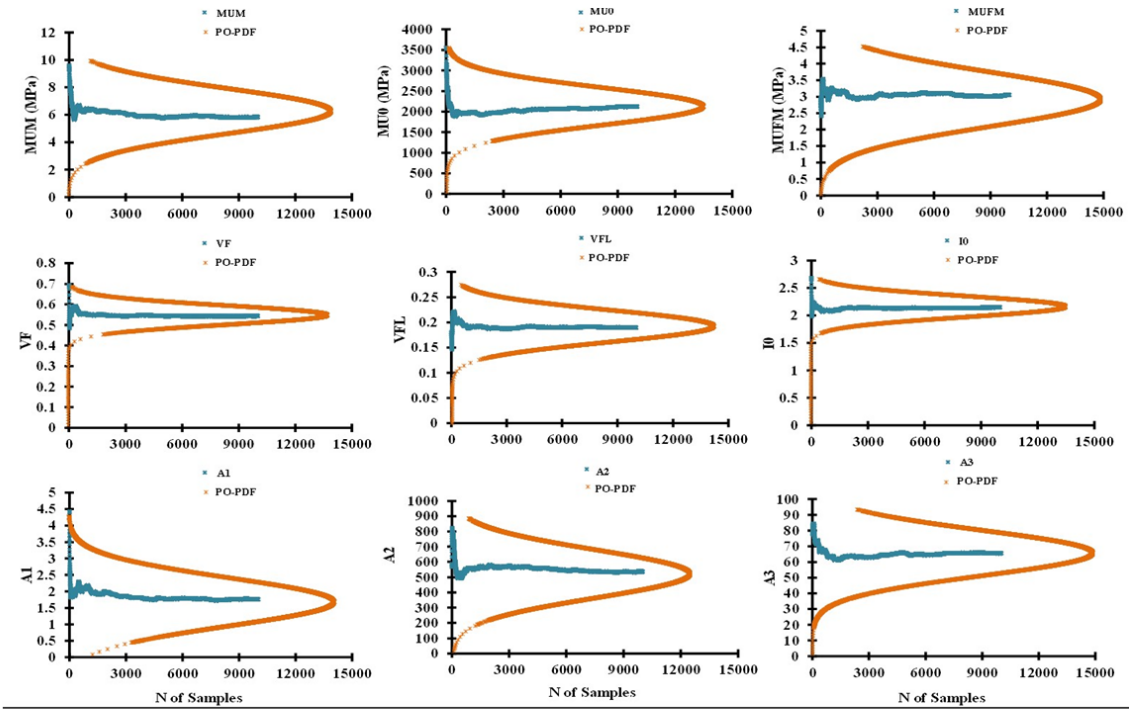


| | MUM | MU0 | MUFM | VF | VFL | I0 | A1 | A2 | A3 |
|---|---|---|---|---|---|---|---|---|---|
| Mean | 5.128 | 2123.135 | 3.047 | 0.543 | 0.189 | 2.143 | 1.751 | 545.048 | 65.439 |
| Std | 1.532 | 449.710 | 0.860 | 0.047 | 0.030 | 0.190 | 0.758 | 162.116 | 14.346 |

LCL

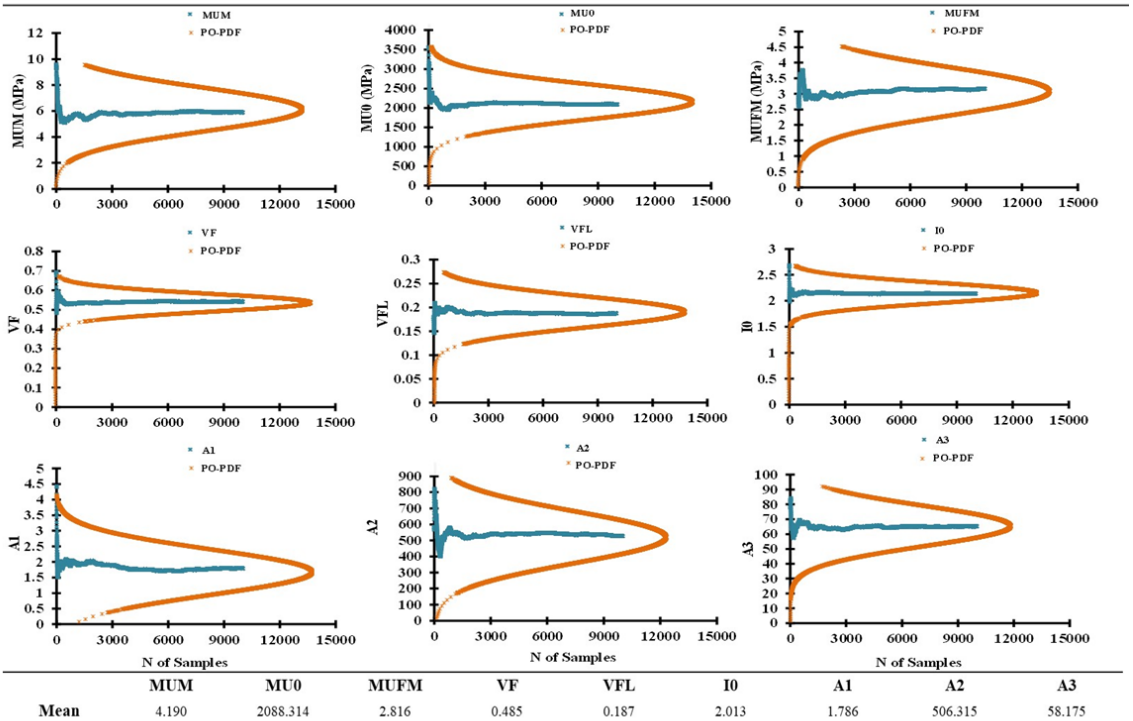


| | MUM | MU0 | MUFM | VF | VFL | I0 | A1 | A2 | A3 |
|---|---|---|---|---|---|---|---|---|---|
| Mean | 4.190 | 2088.314 | 2.816 | 0.485 | 0.187 | 2.013 | 1.786 | 506.315 | 58.175 |
| Std | 1.608 | 432.546 | 0.789 | 0.047 | 0.031 | 0.192 | 0.774 | 164.294 | 13.521 |

Fig. 2 Posterior probability distribution function (PO-PDF) and mean of calibrated material parameters (Bayesian calibration with 10000 MCMC). $\mu_m$ (MUM) Shear modulus of the ligament matrix, $\mu_0$ (MU0) Shear modulus of the fibril, $\mu_{fm}$ (MUFM) Shear modulus of the fiber matrix, $v_f$ Volume fraction of the fibre, $v_{fl}$ Volume fraction of the fibril, $I_0$ Secondary stiffening of the fibril, $a_i$ Dimensionless fibril parameters

**Model calibration:** By considering the above-proposed model, 13 parameters (unknowns) were orchestrating the micro and macro mechanical behavior of the knee connective tissues and most of them related to fibril and fiber properties. A statistical calibration is followed to find the unknown probability distribution function (PDF) of these parameters (MATLAB 2017a, the MathWorks, Natick, 2017). The experimental data (normal stresses) used in this study are taken from the mean (STD) data of in vitro measurements uniaxial tensile failure test [16]. In the Butler study, each sample consist of Bone-Ligament-Bone (BLB) structure was mounted in a test chamber, to reduce the water loss, of an Instron testing machine where the failure test was conducted at high strain rate (100% and 50% s-1). Thereafter, the nominal stress was measured using an axial load cell. From the above experimental data, only four equidistant points are considered here as the targeted calibration data with D = ($d_1$ ($\mu_1, \sigma_1$), $d_2$ ($\mu_2, \sigma_2$), $d_3$ ($\mu_3, \sigma_3$), $d_4$ ($\mu_4, \sigma_4$)), where $\mu_i$ and $\sigma_i$ refers to the mean and the standard deviation of the nominal stress.

In order to permit extensive exploration of the parameters, space radial basis function (RBF) was considered as an approximation of simulation responses (a Meta model created based on FE simulation). In this investigation, $G_{i(1\to4)}(\boldsymbol{\theta})$ refers to the RBF approximation of the nominal stress as a function of the unknown material parameters. The difference between the RBF approximation and the experimental target points were considered as the likelihood function driven Markov Chain Monte Carlo (MCMC) approach, which is used numerically to figure out the posterior distribution (PDF); representing the Bayesian formulation used during this investigation to calibrate the proposed model.

**Collateral ligaments model:** The MCL and LCL geometry was obtained from a three dimensional whole knee-joint model from the OpenKnee public domain repository at Simtk.org [17]. The model generated from a right cadaveric knee of a female subject, 70 years old, 170 cm height and 77 kg. The knee specimen was imaged at the Biomechanics laboratory of the Cleveland Clinic using a 1.0 Tesla extremity MRI scanner. This geometry was then imported into Ansys 19 (Ansys, Inc, Pennsylvania, United States) a finite element package in which an extensive mesh was implemented. Continuum-

based reduced integration eight-node hexahedral elements were used to represent the ligaments (5837 elements). A local elements system axes were created to allow accurate incorporation of collagen networks through ligament structures. To examine the validity of the calibrated material model, additional simulations were carried out using the above realistic geometry of the knee ligaments. The boundary conditions were considered here to mimic a realistic map of loading. Here, LCL and MCL experienced a regular failure tensile testing where the axial load was paralleled to the axis of the ligament.

## III. Results

To figure out the unknown parameters of the multiscale ligaments model, nominal stress and yielding stress during failure tensile test were competed to fit the experimental data [16] statistically. Under low or regular loading condition (max 10% applied strain), the resulting mean and standard deviation of the parameters, governing the material model of the ligaments, derived from the 10000 MCMC simulations are shown in Fig. 2. With the maximum likelihood set of material parameters and those for the selected set of data used during the Bayesian calibration (4 points), the computed nominal stresses lie well with the experimental measurement. Thus, the rest of the measured nominal stresses were fitted well by our prediction (Fig. 3). The coefficients of determination ($R^2$) were 0.96 and 0.93 for the selected set of data used during calibration and the all experimental data considered as a reference during the tensile test, respectively.

At full extension and under pre-yielding loading condition (max 10% axial load), the ligaments stress/strain was nonuniform at all loading stages (Fig. 4). MCL tensile stress/strain reaches their maximal value of 22 MPa at 10% in the anterior femoral insertion. The middle bundle supported most of the load carried by the LCL. During the failure test and when the cross-link density β run between seven and nine, the predicted yielding stress/strain match the experimental measurement (Figs. 3 and 5). The stiffness of the ligaments under axial tension increased significantly by increasing the cross link-density between the tropocollagen molecules (Fig. 5). The stress-strain behavior of the maximal ligaments stress showed three different regions before fiber failure. The toe region is characterized by small stiffness followed by gradual transition and a linear stiffer region.

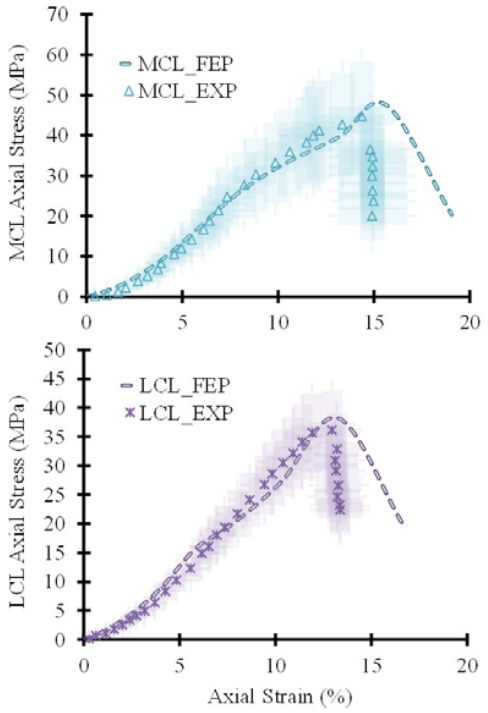


Fig. 3 The total set of experimental data of nominal stress measured from the tensile test (EXP) [16], along with FE model predictions

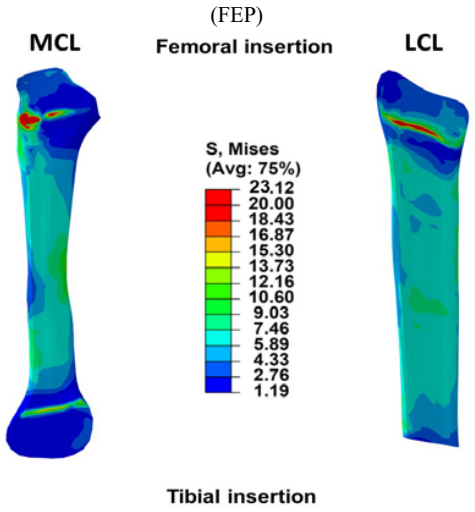


Fig. 4 Von Mises stress distribution in the collateral ligaments at 10% axial tensile test

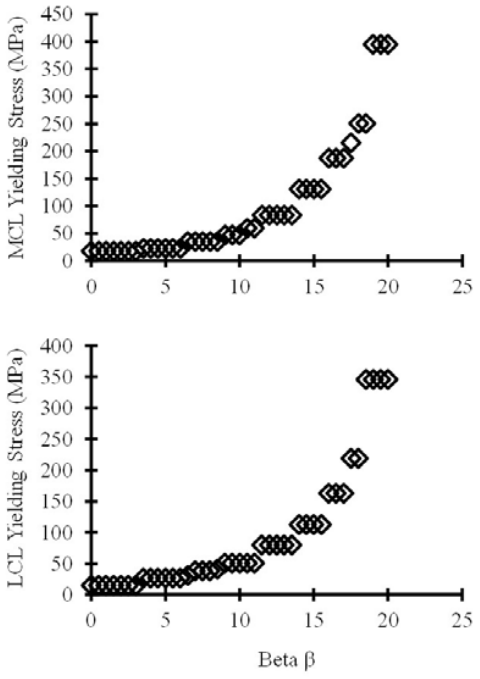


Fig. 5 Collateral ligaments yield strength prediction under varied cross-link density (β) of the tropocollagen molecules

## IV. Discussion

This work was performed as a first step to delineate the interaction between the micro- and macro-scale properties of the collateral ligaments (MCL and LCL) under isolated and physiological loading conditions. For this purpose, a multiscale fibril reinforced hyper-elastoplastic model accounting for the structural architecture of the soft tissue, starting from tropocollagen molecule that forms fibril to whole soft tissue [13], was developed, while driven by reported experimental data of failure tensile test [16]. Unknown material parameters and ligaments detailed response are computed following a statistical calibration procedure yielding results that satisfied experimental data measured during failure tensile tests while accounting nonlinear properties as a function of molecular characteristic.

The employed ligaments FE model was characterized by a set of defined material parameters. Some of these parameters were obtained directly from the literature, while others were computed from a statistical procedure to fit experimental data [16]. The parameters taken from previously published works were related directly to the micro- and macro-scale behavior of the connectives tissues and widely validated from experimental to modeling investigations [13]-[15], [18]. For the rest of the determined parameters, only a few or no data were available in the literature. These calibrated parameters led to a stress-strain curve of the collagen fiber in satisfactory agreement with the former experimental and modeling investigations [19]-[22]. For the cross-link density parameter (β), no published data are available. The lowest value of cross-link density between the tropocollagen molecules was computed for the lateral collateral ligaments (7.5 equivalent strength 1018 MPa). This density increased with MCL and reached 9.5 (equivalent strength 1392 MPa). After that, the predicted posterior distributions (PDF) of the model parameters were in good qualitative and quantitative agreement with published studies.

MCL and LCL Ligaments yield strength, as well as stiffness, are influenced by the cross-link density between tropocollagen molecules (Fig. 5). The range of elasticity of the connective tissues substantially increases when the cross-link density becomes greater than six, this is due to the relative augmentation in the fibrils yield strength. Former observations were reported in the literature to explain the slight increase of the tendon stiffness and strength with aging by the relative elevation in the cross-link density [23], [24]. Our predicted patterns of microdamage (plastic change) are in line with previously reported ligaments failure patterns [25], [26].

In conclusion, the current novel multiscale fibril reinforced hyper elastoplastic FE model that accounts for the synergy between atomistic and continuum syntheses was used to determine the short-term stress/strain collateral ligaments response. To the best of our knowledge, this is the first attempt to model a ligament from the bottom up, in which prediction is dependent on tropocollagen cross-link density. We argue that such a modeling effort can be extended to explore and understand some pathologies and can be used to guide contemporary tissue engineering principles.

## Acknowledgment

Supported by a grant from the Australian College of Kuwait.

## References

[1] Almekinders, L. C. and A. J. Banes, *Tendon and Ligaments*, in *Human Cell Culture*. 2001, Springer. p. 17-25.
[2] Amiel, D., et al., *Tendons and ligaments: a morphological and biochemical comparison.* Journal of Orthopaedic Research, 1983. 1(3):

p. 257-265.
[3] Gardiner, J. C. and J. A. Weiss, *Subject-specific finite element analysis of the human medial collateral ligament during valgus knee loading.* J Orthop Res, 2003. 21(6): p. 1098-106.
[4] Gardiner, J. C., J. A. Weiss, and T. D. Rosenberg, *Strain in the human medial collateral ligament during valgus loading of the knee.* Clin Orthop Relat Res, 2001. 391(391): p. 266-74.
[5] Weiss, J. A. and J. C. Gardiner, *Computational modeling of ligament mechanics.* Crit Rev Biomed Eng, 2001. 29(3): p. 303-71.
[6] Lorentzon, R., H. Wedrèn, and T. Pietilä, *Incidence, nature, and causes of ice hockey injuries: a three-year prospective study of a Swedish elite ice hockey team.* The American journal of sports medicine, 1988. 16(4): p. 392-396.
[7] Najibi, S. and J. P. Albright, *The use of knee braces, part 1: prophylactic knee braces in contact sports.* The American journal of sports medicine, 2005. 33(4): p. 602-611.
[8] Warme, W. J., et al., *Ski injury statistics, 1982 to 1993, Jackson Hole ski resort.* The American journal of sports medicine, 1995. 23(5): p. 597-600.
[9] Grood, E., et al., *Ligamentous and capsular restraints preventing straight medial and lateral laxity in intact human cadaver knees.* JBJS, 1981. 63(8): p. 1257-1269.
[10] Kennedy, J., et al., *Tension studies of human knee ligaments. Yield point, ultimate failure, and disruption of the cruciate and tibial collateral ligaments.* The Journal of bone and joint surgery. American volume, 1976. 58(3): p. 350-355.
[11] Blankevoort, L. and R. Huiskes, *Ligament-bone interaction in a three-dimensional model of the knee.* J Biomech Eng, 1991a. 113(3): p. 263-9.
[12] Orozco, G. A., et al., *The effect of constitutive representations and structural constituents of ligaments on knee joint mechanics.* Scientific reports, 2018. 8(1): p. 2323.
[13] Tang, H., M. J. Buehler, and B. Moran, *A constitutive model of soft tissue: from nanoscale collagen to tissue continuum.* Ann Biomed Eng, 2009. 37(6): p. 1117-30.
[14] Tang, Y., et al., *Deformation micromechanisms of collagen fibrils under uniaxial tension.* J R Soc Interface, 2010. 7(46): p. 839-50.
[15] Buehler, M. J. and R. Ballarini, *Materiomics: multiscale mechanics of biological materials and structures*. 2013: Springer.
[16] Butler, D. L., M. D. Kay, and D. C. Stouffer, *Comparison of material properties in fascicle-bone units from human patellar tendon and knee ligaments.* J Biomech, 1986. 19(6): p. 425-32.
[17] Erdemir, A., *Open knee: open source modeling & simulation to enable scientific discovery and clinical care in knee biomechanics.* The journal of knee surgery, 2016. 29(2): p. 107.
[18] Dhaher, Y. Y., T. H. Kwon, and M. Barry, *The effect of connective tissue material uncertainties on knee joint mechanics under isolated loading conditions.* J Biomech, 2010. 43(16): p. 3118-25.
[19] Eppell, S., et al., *Nano measurements with micro-devices: mechanical properties of hydrated collagen fibrils.* Journal of the Royal Society Interface, 2006. 3(6): p. 117-121.
[20] Shen, Z. L., et al., *Stress-strain experiments on individual collagen fibrils.* Biophysical journal, 2008. 95(8): p. 3956-3963.
[21] Shen, Z. L., et al., *Viscoelastic properties of isolated collagen fibrils.* Biophysical journal, 2011. 100(12): p. 3008-3015.
[22] Yamamoto, N., *ensile Strength of Single Collagen Fibrils Isolated from Tendons.* European Journal of Biophysics, 2017. 5(1): p. 6.
[23] Couppe, C., et al., *Mechanical properties and collagen cross-linking of the patellar tendon in old and young men.* Journal of applied physiology, 2009. 107(3): p. 880-886.
[24] Gautieri, A., et al., *Age- and diabetes-related nonenzymatic crosslinks in collagen fibrils: candidate amino acids involved in Advanced Glycation End-products.* Matrix Biol, 2014. 34: p. 89-95.
[25] Noyes, F. R., J. L. DeLucas, and P. J. Torvik, *Biomechanics of Anterior Cruciate Ligament Failure: An Analysis of.* J. Bone Joint Surg. Am, 1974. 56: p. 236-253.
[26] Noyes, F. R., et al., *Biomechanics of ligament failure: II. An analysis of immobilization, exercise, and reconditioning effects in primates.* JBJS, 1974. 56(7): p. 1406-1418.